Why Liquid Displacement Methods Are Sometimes Wrong in Estimating the Pore-size Distribution

Anna J. Gijsbertsen-Abrahamse and Remko M. Boom
Wageningen University, Food and Bioprocess Engineering Group, 6700 EV Wageningen, The Netherlands

Albert van der Padt
Friesland Coberco Dairy Foods, Corporate Research, 7400 AB Deventer, The Netherlands

DOI 10.1002/aic.10124
Published online in Wiley InterScience (www.interscience.wiley.com).

The liquid displacement method is a commonly used method to determine the pore size distribution of micro- and ultrafiltration membranes. One of the assumptions for the calculation of the pore sizes is that the pores are parallel and thus are not interconnected. To show that the estimated pore size distribution is affected if this assumption is not satisfied, we developed two models: (1) a model describing the flow through an isotropic porous membrane with uniform pores, and (2) a two-layer model for uniform pores that approximates the first model if the membrane thickness is larger than 10 times the pore radius. In the two-layer model the membrane skin layer is divided into two parts: the unconnected pore layer and a sublayer. This model is extended to describe pore activation as a function of pressure with a pore size distribution in the unconnected pore layer (that is, membrane surface). It is shown that, depending on the membrane thickness or the sublayer resistance, the transmembrane pressure needs to be much larger than the critical pressure of the pores, to activate all the pores. If the sublayer resistance is over 10% of the resistance of the unconnected pore layer, the pore size is underestimated with the liquid displacement method; thus the number of pores is overestimated. Because the sublayer resistance is always larger than the unconnected pore layer resistance in an isotropic membrane with interconnected pores, we conclude that the estimated pore size distribution is always shifted toward smaller pore sizes than they really are. To use the liquid displacement method correctly, we suggest either counting the number of (active) pores or measuring the flux–pressure curve several times, while covering each time a different fraction of the membrane surface. *AIChE J,* 50: 1364–1371, 2004
Keywords: liquid displacement method, pore size distribution, interconnected pores, resistance, flux

Introduction

To characterize filtration membranes, several methods have been developed to determine pore size, pore size distribution, and porosity. They can be classified into: (1) methods to determine pore size and pore size distribution of a membrane and (2) methods based on rejection performance using reference molecules and particles (Nakao, 1994). The liquid displacement method, falling under class 1, is commonly used to determine membrane pore size distributions because it is close to (ultra)filtration practice: dead-end pores are not evaluated; the membrane is characterized in wet conditions; in addition the pressure is kept as low as possible and thus no alteration of the membrane occurs (Nakao, 1994). The method was first described by Erbe (1933) and Kesting (1971) and further developed by Capannelli et al. (1983, 1988). It is based on the measurement of the flux of a displacing liquid through the

Correspondence concerning this article should addressed to A. J. Gijsbertsen-Abrahamse at this current address: Kiwa Water Research, P.O. Box 1072, 3430 BB Nieuwegein, The Netherlands (e-mail: anneke.gijsbertsen@kiwa.nl).

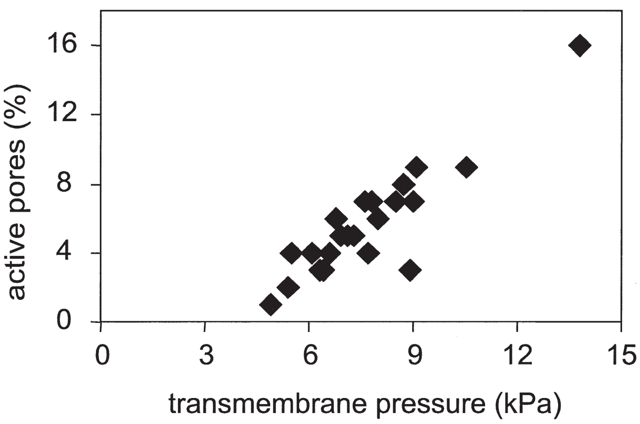

Figure 1. Percentage of active pores as a function of the transmembrane pressure in microsieve emulsification experiments (Abrahamse et al., 2002).

membrane as a function of the pressure applied. From the flux–pressure curve the pore size distribution is calculated using the Hagen–Poiseuille equation. Although many researchers investigated the liquid displacement method and improvements were suggested (Piatkiewicz et al., 1999; Vaidya and Haselberger, 1994; Wienk et al., 1994), no one studied how the pore size distribution determination is affected by pore connections (that is, if the pores are not straight through the whole membrane layer). Nevertheless, the method is not only used to determine the pore size distribution of membranes with straight-through pores (Jakobs and Koros, 1997; Kujawski et al., 1989; Munari et al., 1985, 1989), but also for symmetric membranes and asymmetric membranes with a thin skin layer characterized by more or less interconnecting pores (Bottino et al., 1991, 1994; Capannelli et al., 1983; Mikulášek and Dolecek, 1994; Munari et al., 1985).

In emulsification experiments with micromachined membranes having exactly monodisperse pores (microsieves) we found that to open up the pores the transmembrane pressure had to be increased (Figure 1; Abrahamse et al., 2002). Membrane emulsification is quite similar to the liquid displacement method because one fluid (oil) is pressed through the membrane pores into another fluid (emulsifier solution). Figure 1 shows that, even at transmembrane pressures of several times the critical pressure of these pores, only a small fraction of pores opened up. If this would have been a liquid displacement experiment, it would have been concluded that the membrane had a wide distribution, which is in contrast with the uniform pore sizes. We showed that the gradual increase in pore activation could be attributed to the presence of an extra resistance against flow below the parallel top layer pores (Gijsbertsen-Abrahamse et al., 2003). Furthermore, we found that if the pores within the membrane skin layer are interconnected, this leads to the same effect as described above: the lower side of the skin layer acts as an extra resistance below the pores that open up to the downstream side of the membrane. In experiments with a ceramic membrane of 150 μm thickness the activation of pores with increasing transmembrane pressure was very gradual (Gijsbertsen-Abrahamse et al., 2003). This could not be attributed to pore size differences only because if we consider the transmembrane pressures at which oil started to flow through the pores, then the pores that became active at higher pressures would have been several times smaller than the first active pore. Given that only a very small fraction of the pores was studied ($<0.2\%$), it is not convincing that the diameters will have differed so much. Therefore, we come to the conclusion that indeed part of the membrane skin layer could be interpreted as a sublayer resistance.

In this article we show that the apparent pore size distribution obtained is strongly influenced by the interconnections of the membrane pores; the apparent pore size distribution will be shifted to much smaller sizes compared to that of the real distribution. First, the main points and assumptions of the liquid displacement method are recapitulated. Then flow through an isotropic membrane with uniform pores is modeled, and the effect of a pore size distribution of the surface pores is represented in a two-layer model: the membrane skin layer is assumed to be divided in an unconnected pore layer and a sublayer. Furthermore, we suggest two methods to modify the liquid displacement method to take pore connections into account.

Theory of the Liquid Displacement Method

The liquid displacement method is an indirect method for determination of the pore size distribution of a membrane because first a flux–pressure curve is measured, from which the pore size distribution is subsequently calculated. To measure the flux–pressure curve a pair of immiscible liquids with a low interfacial tension is used. The membrane is wetted with one of the liquids. By a stepwise increase of the transmembrane pressure, the nonwetting liquid is pressed through the membrane. With increasing pressure, first the liquid in the largest pores is displaced, then, at higher pressures, increasing numbers of smaller pores are opened (Capannelli et al., 1983; Erbe, 1933; Kesting, 1971). Eventually, a pressure is reached at which further increases result only in an increase in flux that is proportional to the increase in pressure (Kesting, 1971). Alternatively, a low surface tension liquid may be displaced by pressurized nitrogen to characterize microfiltration membranes. From the flux–pressure curve the pore size distribution can be calculated assuming the following (Erbe, 1933):

(1) The pores are cylindrical.

(2) The pores are parallel to each other and not interconnected and are thus straight through the whole membrane layer.

(3) The pores all have a length l, where l is usually taken to be the thickness of the membrane (or the thickness of the membrane skin layer in the case of an asymmetric membrane) (Capannelli et al., 1983; Munari et al., 1989).

With assumption 2 (parallel pores), and the implicit assumption that nowhere in the measuring setup is a resistance against flow present, the transmembrane pressure at which the liquid in a pore is displaced is equal to the critical pressure of that pore. Assuming a cylindrical pore (assumption 1), the critical pressure of a pore can be calculated with the Laplace equation

$$p_{crit} = \frac{2\gamma \cos \theta}{r_p} \qquad \text{(Pa)} \tag{1}$$

in which γ is the interfacial tension between the two liquid phases, r is the radius of the pore, and θ is the wall contact

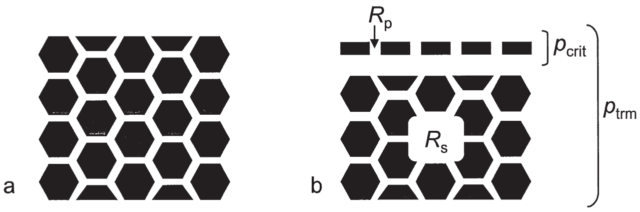

Figure 2. (a) Isotropic membrane with uniform pores; (b) two-layer model for uniform pores.

angle. For convenience, usually the contact angle θ is taken to be zero. Actually, this is the only value giving correct results in the case of pores with sharp edges because the droplet always has to go through the hemispherical stage (Gijsbertsen-Abrahamse et al., 2002; Piatkiewicz et al., 1999). In that stage the pressure is maximal and can be calculated with

$$p_{crit} = \frac{2\gamma}{r_p} \qquad \text{(Pa)} \tag{2}$$

With assumptions 1 and 3, the number of pores in a certain size class (N) can be calculated from the increase in the measured flux ($d\phi_s$) upon the increase in transmembrane pressure (dp_{trm}) (see, for example, Capannelli et al., 1983; Erbe, 1933; Kesting, 1971):

$$N(r_p) = \frac{8\eta l}{\pi r_p^4} \frac{d\phi_s}{dp_{trm}} \tag{3}$$

where η is the viscosity of the displacing liquid. If l is not known, a relative pore size distribution can be calculated.

Effect of Interconnected Pores on Pore Size Estimation

Most membranes are not characterized by parallel, unconnected pores. Most symmetric membranes have highly interconnected, tortuous pores, as is the case for the skin layer of asymmetric membranes (Figure 2a). In this section we will show that this has a strong effect on the estimation of the pore size distributions by liquid displacement. In the first section we will model the flux–pressure curve with an isotropic membrane model. Then the similarity between this model and a simpler two-layer model for uniform pores is shown (schematically in Figure 2b). The two-layer model was developed to describe pore activation in membrane emulsification (Gijsbertsen-Abrahamse et al., 2003). Finally, to include the effect of different pore sizes in the model, the two-layer model is extended.

Isotropic membrane model

To determine the effect of pore connections, the flux through an isotropic membrane with uniform pores (equal pore radii and pore lengths) is calculated as a function of the transmembrane pressure and the membrane thickness. Figure 3 shows that increasing numbers of pores are activated upon increasing transmembrane pressure. Because of the flow through an active pore, the pressure just below that pore drops to a value lower than the critical pressure and the pressures below the pores

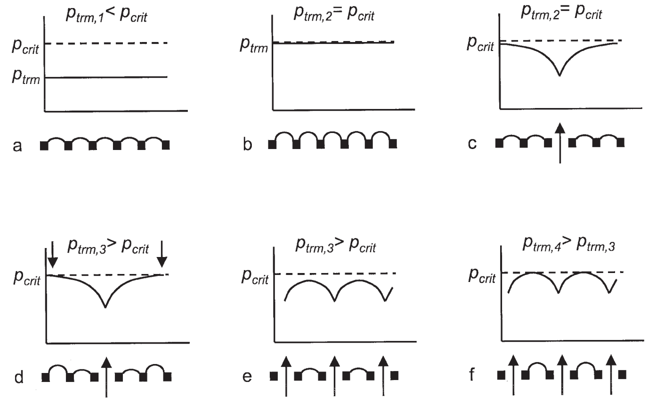

Figure 3. Gradual activation of pores with increasing transmembrane pressure (p_{trm}) (on the *x*-axes, the position of the surface pores; on the *y*-axes, the pressure just below the surface pores).

Surface pores, where either a droplet is present or the pore is active (depicted by arrows).

close to the active pore also decrease (Figure 3c). The pressure decreases least under the pores that are farthest away from an active pore; these pores will be activated next (Figure 3d). With this in mind, we assumed that the space around an already active pore can be approximated by a cylinder (Figure 4). The pressure under the surface pores at the edge of the cylinder and the flux through the cylinder were calculated as a function of the cylinder radius and the membrane thickness. From these results, the fraction of active pores and the flux can be determined as a function of the membrane thickness and the ratio of the transmembrane pressure and the critical pressure of the pores.

The Model. Analogous to the model of Ho and Zydney (1999) for pore blockage during filtration, we modeled the pressure profile in the cylindrical part of the porous membrane (Figure 4b). With Darcy's law and the continuity equation, a second-order partial differential equation for the local pressure is obtained (Ho and Zydney, 1999)

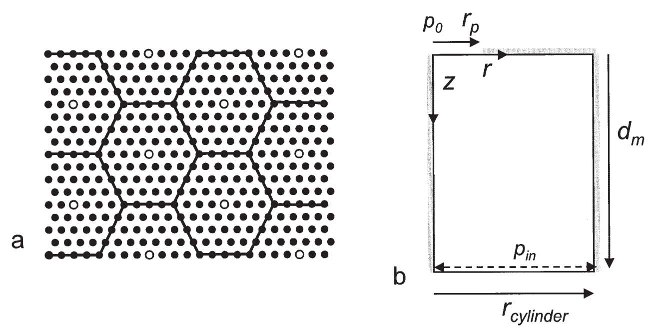

Figure 4. (a) Top surface of a membrane with active pores (○) and nonactive pores (●); (b) approximation of the hexagon around an active pore in (a) by a cylinder.

Dimensions and boundary conditions are shown (in gray boundary conditions: $\partial p/\partial r = 0$ or $\partial p/\partial z = 0$). Symbols are explained in the notation section.

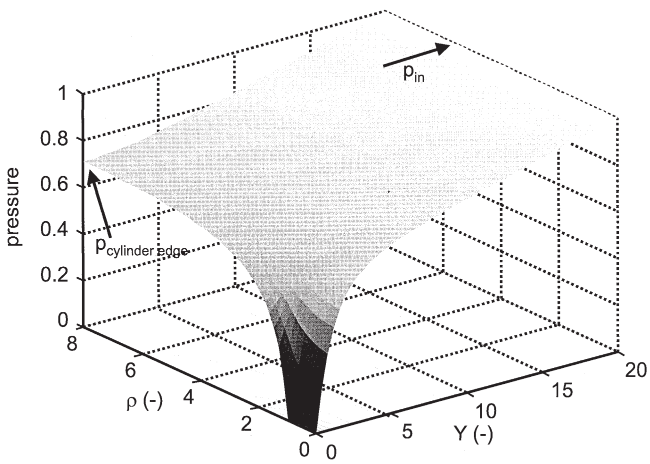

Figure 5. Pressure profile in a cylinder (p_{in} = 1, p_0 = 0, ρ_{cyl} = 8, δ_m = 20).

$$\frac{k_r}{r}\frac{\partial}{\partial r}\left(r\frac{\partial p}{\partial r}\right)+k_z\frac{\partial^2 p}{\partial z^2}=0 \qquad (\mathrm{s}^{-1}) \tag{4}$$

in which k_r and k_z are the permeabilities in the radial and transverse directions, respectively.

The boundary conditions are given by

$$r=0: \qquad \frac{\partial p}{\partial r}=0 \tag{5}$$

$$r=r_{cylinder}: \qquad \frac{\partial p}{\partial r}=0 \tag{6}$$

$$z=d_m: \qquad p=p_{in}=p_{trm}+p_0 \tag{7}$$

$$z=0: \qquad p=p_0 \qquad 0\le r\le r_p \tag{8a}$$

$$\frac{\partial p}{\partial z}=0 \qquad r_p<r\le r_{cylinder} \tag{8b}$$

We assume an isotropic membrane, implying equal permeabilities in the radial and transverse directions: $k_r = k_z$, and thus they both can be removed from Eq. 4. The problem was nondimensionalized in the radial and transverse directions using the pore radius (r_p): $\rho = r/r_p$ and $Y = z/r_p$, so $\rho_{cyl} = r_{cylinder}/r_p$ and $\delta_m = d_m/r_p$. A typical result of the pressure profile in the cylinder is shown in Figure 5 ($\rho_{cyl} = 8$, $\delta_m = 20$, $p_{in} = 1$, $p_0 = 0$).

Results. In Figure 6a the ratio of the transmembrane pressure ($p_{trm} = p_{in} - p_0$) and the pressure under the pores at the edge of the cylinder is shown as a function of the cylinder radius and the membrane thickness. A decreasing cylinder radius means that the distance between active pores decreases and the fraction of active pores increases. To activate a pore, the pressure under the pore should be equal to the critical pressure. Figure 6a thus shows that to increase the number of active pores, the transmembrane pressure should substantially increase. This is shown in Figure 3. In the case of a membrane with a dimensionless thickness of 80, the transmembrane pressure should even be increased to about 70 times the critical pressure to activate all the pores.

The fraction of active pores (n) at a certain ratio of transmembrane pressure and critical pressure, was calculated by

$$n\big|_{p_{trm}/p_{crit}}=\frac{A_{active}}{A_m}=\frac{\pi r_p^2}{\pi(0.5r_{cylinder})^2}=\left(\frac{1}{0.5\rho_{cyl}}\right)^2 \tag{9}$$

The value of n was calculated using $0.5{\cdot}\rho_{cyl}$ because it was assumed that at the value of p_{trm}/p_{crit} (calculated using ρ_{cyl}), some pores at the edge of the cylinder just become active. Thus, the distance between two active pores was reduced to half the cylinder radius. n is plotted as a function of $(p_{trm}/p_{crit}) - 1$ divided by the dimensionless membrane thickness (δ_m) (Figure 6b). With this figure it is clearer that to activate all the pores, the transmembrane pressure should be many times the critical pressure, depending on the membrane thickness, even for uniform pores! Because the transmembrane pressure at which a pore becomes active is no longer only a function of the pore radius, using the liquid displacement method will introduce errors in the estimation of the pore size distribution. To estimate these errors, we calculated the flux–pressure curves using the following equation to determine the pressure gradient at the bottom of the cylinder

$$\left.\frac{\Delta p}{\Delta Y}\right|_{p=p_{in}}=\int_0^{\rho_{cyl}}\left.\frac{\Delta p}{\Delta Y}\right|_{Y=\delta_m}d\rho \qquad (\mathrm{Pa}) \tag{10}$$

From this pressure gradient the flux of the nonwetting liquid phase was calculated according to Darcy's law

$$\phi_s=A_mk_z\left.\frac{\Delta p}{\Delta Y}\right|_{p=p_{in}}\frac{1}{r_p}=A_mk_z\left.\frac{\Delta p}{\Delta Y}\right|_{p_{crit}=1}\frac{p_{crit}}{r_p} \qquad (\mathrm{m^3/s}) \tag{11}$$

in which A_m is the membrane area considered, and k_z can be written as K/η; K is the permeability (in m^2) and can be determined by measuring the membrane flux and using the Hagen–Poiseuille equation or the Kozeny–Carman equation (Mulder, 1991). The permeability, and thus the flux, will be a function of the membrane porosity. Figure 7a–b shows the flux–pressure curves of two membranes with the same uniform pore size, but different thicknesses, and the apparent pore size distributions estimated with the liquid displacement method

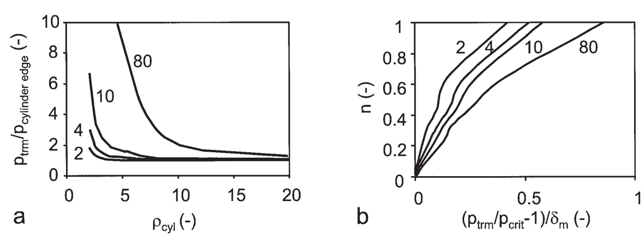

Figure 6. Results obtained with the isotropic membrane model with several membrane thicknesses.

(a) Ratio of transmembrane pressure and the pressure under the pores at the edge of the cylinder as a function of the dimensionless cylinder radius; (b) fraction of active pores as a function of the dimensionless pressure divided by δ_m.

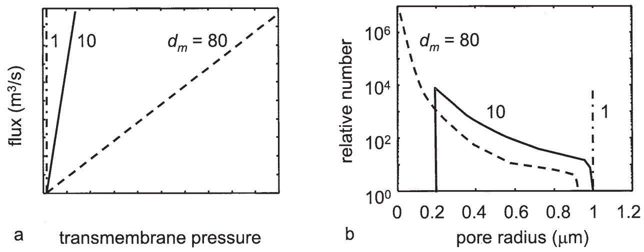

Figure 7. (a) Flux–pressure curves calculated with the isotropic membrane model [r_p = 1 μm (K = 1.8 × 10^{-14} m²), d_m = 1, 10, and 80 μm]; (b) original pore-size distribution and pore-size distributions estimated from the flux–pressure curves in (a) with the liquid displacement method.

(described in the section theory) from those flux–pressure curves. It is clear that the obtained pore size distributions are not correct: the estimated pore sizes are much too small. The thicker the membrane compared to the pore radius, the worse the estimation of the pore size distribution.

Isotropic membrane model and two-layer model compared

Both the fraction of active membrane surface pores and the pressure gradient at the bottom of the cylinder are roughly linearly dependent on the dimensionless transmembrane pressure (Figures 6b and 8). This is especially true for the flux, which is approximately linearly dependent on the pressure gradient when $\delta_m > 10$. These linear dependencies substantially resemble the two-layer model, developed to describe pore activation in membrane emulsification (Gijsbertsen-Abrahamse et al., 2003). In the two-layer model, the membrane is assumed to be composed of two distinct structural layers: an unconnected pore layer having parallel pores and a sublayer, with each layer having a given resistance to fluid flow (Figure 2b). In the next section it will be shown that the two-layer model can easily be extended to describe the effect of different pore sizes on the estimation of the pore size distribution. Therefore, in this section we compare the two models and give equations to convert the isotropic membrane model in the two-layer model.

In the two-layer model for uniform pores, the number of active pores (N) is given by

$$N = \frac{R_p}{R_s}\left(\frac{p_{trm}}{p_{crit}} - 1\right) \tag{12}$$

in which R_p is the resistance of a single pore in the unconnected pore layer and R_s is the resistance of the sublayer, which is in series with the unconnected pores. The fraction of active pores (n) is calculated by dividing both N and the single pore resistance (R_p) by the total number of pores in the surface (N_{tot})

$$n = \frac{N}{N_{tot}} = \frac{R_p/N_{tot}}{R_s}\left(\frac{p_{trm}}{p_{crit}} - 1\right) = \frac{R_{up}}{R_s}\left(\frac{p_{trm}}{p_{crit}} - 1\right) \qquad (N < N_{tot}) \tag{13}$$

in which R_{up} is the total resistance of the pores in the unconnected pore layer. The ratio of resistances R_{up}/R_s for a membrane with interconnected pores can now be calculated from the slopes (a) of the graphs in Figure 6b, in which n is shown as a function of $[(p_{trm}/p_{crit}) - 1]/\delta_m$ and thus

$$\frac{R_{up}}{R_s} = \frac{a}{\delta_m} = \frac{ar_p}{d_m} \tag{14}$$

The value of a ranges from around 2 for a very thin membrane to 1 for a thick membrane. This means that R_{up}/R_s is always smaller than 1 for a membrane with interconnected pores. From this result it will be concluded in the next section that the estimation of the pore size distribution with the liquid displacement method is always incorrect with such a type of membrane, as is already partly shown in Figure 7.

To make an estimation of R_s of a membrane with interconnected pores, the equation for the flux in the two-layer model

$$\phi_s = \frac{p_{trm}}{\eta R_s} - \frac{p_{crit}}{\eta R_s} = \frac{p_{crit}}{\eta R_s}\left(\frac{p_{trm}}{p_{crit}} - 1\right) \qquad (\mathrm{m^3/s}) \tag{15}$$

should be substituted in the flux equation of the isotropic membrane model (Eq. 11), giving

$$\left.\frac{\Delta p}{\Delta Y}\right|_{p_{crit}=1} = \frac{r_p}{R_s A_m K}\left(\frac{p_{trm}}{p_{crit}} - 1\right) \tag{16}$$

Now the resistance of the sublayer R_s can be calculated from the slopes (b) of the graphs in Figure 8

$$R_s = \frac{r_p}{A_m K}\frac{\delta_m}{b} = \frac{d_m}{A_m K b} \qquad (\mathrm{m^{-3}}) \tag{17}$$

The value of b is close to 1 and is not dependent on the membrane thickness as long as the membrane thickness is more than 10 times the pore radius ($\delta_m > 10$). This implies that in a microfiltration membrane, with a maximum average radius of

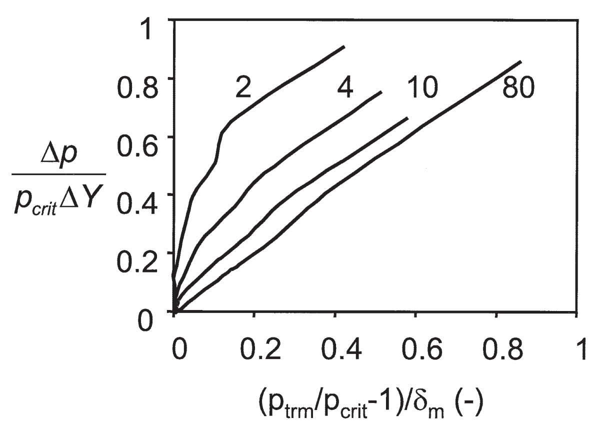

Figure 8. Dimensionless pressure gradient at the bottom of the cylinder, as a function of the dimensionless pressure divided by δ_m, until the point where n = 1.

2.5 μm and a thickness (of the skin layer) of 25 μm, the two-layer model can be used instead of the isotropic membrane model. Usually the membrane or membrane skin layer will be thicker or the pore radius will be smaller; thus in most cases pore activation and the flux–pressure curve can be determined by the two-layer model.

Two-layer model with pore-size distribution

Because the isotropic membrane model is not convenient for determining the effect of interconnected pores on the estimation of the pore size distribution if the pores are not uniform, the two-layer model is extended to describe flow through an unconnected pore layer with pores that are not uniform, and a sublayer. In the preceding section it was shown that in many practical cases the isotropic membrane model can be approximated by the two-layer model.

The Model. The transmembrane pressure necessary to displace the liquid from the *i*th pore can be calculated by assuming that there is no accumulation of fluid in the membrane. Thus, the total flow through the unconnected pore layer (Eq. 18) must equal the flow through the sublayer, described by Eq. 15

$$\phi_{up} = \sum_{i=1}^{N} \phi_p = \frac{p_{crit,i}}{\eta R_{up,i}} \qquad (\mathrm{m^3/s}) \qquad (18)$$

in which ϕ_p is the flux through a pore, ϕ_{up} is the total flux through the unconnected pore layer, and $R_{up,i}$ is the resistance of the unconnected pore layer, which depends on the number and sizes of the pores from which the liquid is displaced, according to Eq. 19

$$R_{up,i} = \frac{1}{\sum_1^i \frac{1}{R_{p,i}}} = \frac{8l}{\pi \sum_1^i r_i^4} \qquad (\mathrm{m^{-3}}) \qquad (19)$$

where l is the unconnected pore length; a best guess for the value of l is probably the diameter of the nodular structure of the membrane. Combining Eqs. 18 and 15 gives

$$p_{trm,i} = p_{crit,i}\left(\frac{R_s + R_{up,i}}{R_{up,i}}\right) \qquad (\mathrm{Pa}) \qquad (20)$$

Hence, the transmembrane pressure at which the liquid from the *i*th pore is displaced is a function of the ratio of the resistance of the two layers ($R_s + R_{up}$) and the resistance in the unconnected pore layer. With this equation it can be explained that even uniform pores do not become active at the same transmembrane pressure. If liquid is displaced from an increasing number of pores, R_{up} decreases and thus the transmembrane pressure needs to be increased to activate additional pores.

Results. In Figure 9a two calculated flux–pressure curves are given: one of a membrane in which the pores (with a log-normal size distribution) are straight through the membrane (or through the skin layer, in the case of an asymmetric membrane) and a membrane with the same log-normal pore size distribution, but with a sublayer resistance in series (calculated with Eqs. 18 and 20). In Figure 9b the pore-size distributions calculated with the commonly used liquid displacement method (described in the theory) are shown. The results clearly show that if a sublayer is present, the determination of the pore size distribution from the flux–pressure curve results in a smaller average pore radius, a larger standard deviation, and a larger number of membrane pores. In the same way we explored different average pore sizes and values of the standard deviation of the pore-size distribution at different values of the sublayer resistance (R_s). The resulting errors in average pore radius, standard deviation, and number of pores using the liquid displacement method are plotted (Figure 10a–10c) as the ratio of the calculated value over the input value. The input is shown on the *x*-axis: the total unconnected pore layer resistance (R_{up}) over the sublayer resistance (R_s).

As long as the sublayer resistance is less than 10% of the resistance of the unconnected pore layer, the membrane can be considered as consisting of just the unconnected pore layer; then the liquid displacement method can be used to determine the pore size distribution without making any errors. However, a larger R_s (with respect to R_{up}) results in an increasing underestimation of the pore radii. As a result, the number of pores is overestimated. From Figure 10b, it follows that the pore size distribution estimated with the liquid displacement method is much wider than it is in reality. This is attributed to the fact that pores with the same radius do not become active at the same transmembrane pressure, which was explained with Eq. 20. In the preceding section it was shown that R_{up}/R_s is always smaller than 1 in a membrane with interconnected pores, which means that the pores cannot be assumed to be straight through the whole membrane layer. Therefore, the liquid displacement method needs to be modified to take the membrane morphology into account, which is discussed below. However, if the membrane is not at all isotropic, $k_r \ll k_z$, or even $k_r = 0$ (which is the case for Nuclepore® track-etched membranes), the liquid displacement method in its original form is correct. Yet, in the two-layer model it is assumed that the liquid is displaced in the pores from the bottom up. However, channeling through the porous matrix may also occur. Then the resistance in the sublayer will be much higher and it cannot be assumed that the pores in the surface layer experience the same critical pressure. Thus in the case of channeling, the model is not valid.

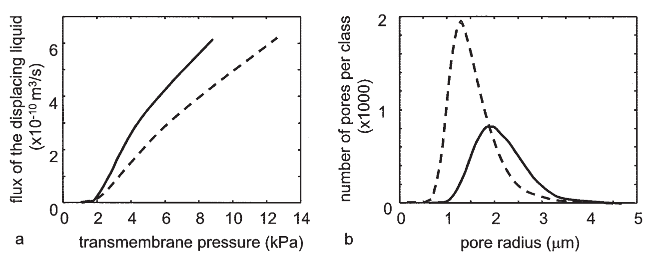

Figure 9. (a) Flux of the displacing liquid as a function of transmembrane pressure for $R_s = 0$ (—) and $R_s = 2 \times 10^{13}$ m^{-3} (- - -); (b) pore size distributions calculated with the liquid displacement method from the flux–pressure curves in (a) (class width 1 × 10^{-7} m).

Values of the original pore size distribution and of the displacing liquid: $\bar{r} = 2 \times 10^{-6}$ m, $\sigma = 0.25$, $n = 1 \times 10^4$, $l = 5 \times 10^{-6}$ m, $R_{up} = 4.77 \times 10^{13}$ m^{-3}, $\gamma = 0.35 \times 10^{-3}$ N/m, $\eta = 30 \times 10^{-3}$ Pa·s.

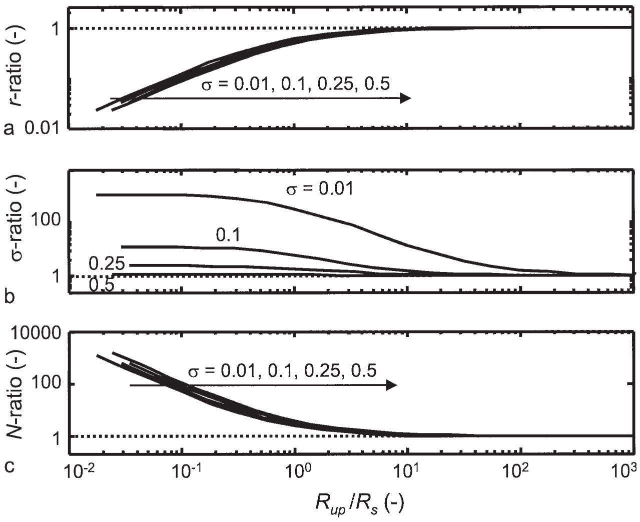

Figure 10. Ratios of the calculated value over the original value as a function of the ratio of the unconnected pore layer resistance (R_{up}) and the sublayer resistance (R_s).

(a) Ratio of the average pore radius; (b) ratio of the standard deviation of the pore size distribution; (c) ratio of the total number of pores. Note that the ratios should be 1 for correct estimation of the pore size distribution (dotted line).

Discussion: Modification of the Liquid Displacement Method

In this section two options are presented to adjust the liquid displacement method, thus including the effects of interconnectivity. In the theory the basis of the liquid displacement method was presented (Eqs. 2 and 3). From the measured flux and pressure vectors, only two of three variables (r, l, and n) can be determined. Therefore, usually l is assumed to have a constant value for all the pores. If a sublayer resistance should be taken into account, there is an extra variable, R_s. To determine the pore size distribution satisfactorily (with the equations given in the preceding section), R_s has to be estimated, either by determination of the number of (active) pores or by repeating the experiment with a partially covered membrane surface. These methods are discussed in more detail in this section.

Determination of the number of (active) pores to estimate R_s

Determination of the number of active pores by visualization would yield the required extra information, although this is not very easy to do. It might be possible to include a microscope in the setup, but observing the displacement of liquid from the smallest pores will be difficult because of the flow of liquid through the other pores. In ultrafiltration membranes it will not be possible to visualize the pores because of their small sizes. Nevertheless with microfiltration membranes, observing only the number of pores from which liquid is displaced in a part of the low pressure range already provides enough information: if it is known exactly to what degree pores cause the measured flux at a certain pressure, the sublayer resistance can be calculated with Eqs. 15 and 18–20. This R_s value can be used to determine the remainder of the pore size distribution. Perhaps one can think of another method to determine the number of active pores as a function of pressure or to determine the total number of pores in the membrane surface. One of these methods would be to increase the transmembrane pressure very slowly and with very small incremental steps to make just one pore active at a time. The flux needs to be measured very accurately because then not only the pressure and flux, but also the number of active pores is known and, again, R_s can be determined.

Repeated flux measurements with partially covered membrane surface to estimate R_s

If the flux, as a function of the transmembrane pressure, is measured several times with different levels of coverage of the membrane surface, different flux–pressure curves are obtained. The covering material could be, for example, a grid with known dimensions. With a metal grid it is also ensured that flexible membranes are sufficiently supported. It is assumed that covering the surface changes only the resistance of the unconnected pore layer (R_{up}) and not R_s. This assumption is probably valid only if the pieces that cover the membrane are not much larger than the average pore radius because, otherwise, a lot of fluid has to flow in the transverse direction through the membrane, resulting in pressure loss. Furthermore, it is expected that the shape of the pore size distribution is not changed by partly covering the membrane, whereas the number of pores will be a fraction of the total number of pores in the unconnected pore layer (f_{uncov} = uncovered area/total membrane area). If there is no sublayer resistance, the flux–pressure curve obtained by partly covering the membrane surface divided by the uncovered fraction coincides with the flux–pressure curve obtained without covering the membrane surface. The flux–pressure curves with different uncovered membrane surface fractions, calculated for the "membrane" in Figure 9, are shown in Figure 11a. Starting at $R_s = 0\ m^{-3}$, the pore size distribution can be estimated from this curve by iteratively changing R_s until the ratio of the number of pores of the distributions is equal to the uncovered fraction (Figure 11b). Note that at this R_s ($=2 \times 10^{13}\ m^{-3}$), the pore size distribution curves divided by the uncovered fraction coincide. In reality statistics are essential for determining the best R_s value.

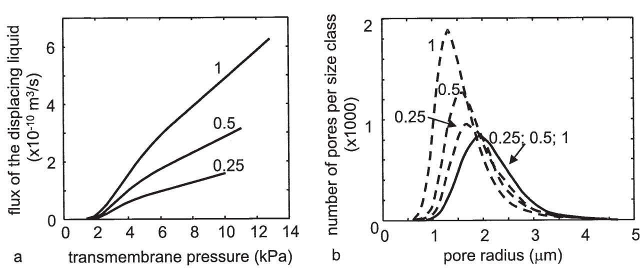

Figure 11. (a) Flux–pressure curves calculated with the two-layer model for a partially covered membrane surface, with $R_s = 2 \times 10^{13}\ m^{-3}$ and further the same data as in Figure 8; (b) pore size distributions estimated with the modified liquid displacement method with $R_s = 0\ m^{-3}$ (—) and $R_s = 2 \times 10^{13}\ m^{-3}$ (- - -), divided by the uncovered fraction.

Numbers denote f_{uncov}.

Conclusions

Determining the pore size distribution with membrane characterization methods using liquid displacement is incorrect if the pores are connected to each other or if there is a resistance against flow in the membrane sublayer or in the measurement apparatus. As a result of the additional resistance, the estimated pore size distribution shifts toward smaller pores and a larger number of pores. To overcome this, two methods are suggested to modify the liquid displacement method: either the sublayer resistance is estimated by determining the number of active pores or by repeated measurement of the flux–pressure curves with different levels of coverage of the membrane surface.

Notation

a = slope
A_m = membrane area, m^2
b = slope
d_m = membrane thickness, m
f_{uncov} = uncovered fraction of the membrane surface
K = membrane permeability, m^2
k = membrane permeability, kg m s^{-1}
l = unconnected pore length, m
N = number of pores
N_{tot} = total number of pores
n = fraction of active pores
p_0 = pressure in the displaced liquid, Pa
p_{in} = disperse phase pressure at the inlet of the system, Pa
p_{crit} = critical pressure, Pa
$p_{cylinder\ edge}$ = pressure at the edge of the cylinder, Pa
p_{trm} = transmembrane pressure, Pa
$r_{cylinder}$ = cylinder radius, m
r_p = pore radius, m
R_p = pore flow resistance, m^{-3}
R_{up} = total resistance of the unconnected pore layer against flow, m^{-3}
R_s = sublayer resistance against flow, m^{-3}
Y = dimensionless axial coordinate

Greek letters

δ_m = dimensionless membrane thickness
ϕ_p = flux of displacing liquid through a pore, m^3/s
ϕ_{up} = flux of displacing liquid through the unconnected pore layer, m^3/s
ϕ_s = total flux of the displacing liquid through the membrane, m^3/s
γ = surface or interfacial tension, N/m
η = viscosity, Pa·s
θ = wall contact angle
ρ = dimensionless radial coordinate
ρ_{cyl} = dimensionless cylinder radius
σ = standard deviation of the pore size distribution

Literature Cited

Abrahamse, A. J., R. van Lierop, R. G. M. van der Sman, A. van der Padt, and R. M. Boom, "Analysis of Droplet Formation and Interactions during Cross-flow Membrane Emulsification," *J. Membr. Sci.*, **204**, 125 (2002).

Bottino, A., G. Capannelli, A. Grosso, O. Monticelli, and M. Nicchia, "Porosimetric Characterization of Inorganic Membranes," *Sep. Sci. Technol.*, **29**, 985 (1994).

Bottino, A., G. Capannelli, P. Petit-Bon, N. Cao, M. Pegoraro, and G. Zoia, "Pore Size and Pore-Size Distribution in Microfiltration Membranes," *Sep. Sci. Technol.*, **26**, 1315 (1991).

Capannelli, G., I. Becchi, A. Bottino, P. Moretti, and S. Munari, "Computer Driven Porosimeter for Ultrafiltration Membranes," *Proc. Studies in Surface Science and Catalysis*, 283 (April 1987).

Capannelli, G., F. Vigo, and S. Munari, "Ultrafiltration Membranes—Characterization Methods," *J. Membr. Sci.*, **15**, 289 (1983).

Erbe, F., "Die Bestimmung der Porenverteilung Nach Ihrer Gröβe in Filtern und Ultrafiltern," *Kolloid-Zeitschrift*, **63**, 277 (1933).

Gijsbertsen-Abrahamse, A. J., A. van der Padt, and R. M. Boom, "Membrane Emulsification: The Influence of Pore Geometry and Wall Contact Angle on Process Performance," in *Proc. CME3,* Lyon, France (Sep. 2002).

Gijsbertsen-Abrahamse, A. J., A. van der Padt, and R. M. Boom, "Influence of Membrane Morphology on Pore Activation in Membrane Emulsification," *J. Membr. Sci.*, **217**, 141 (2003).

Ho, C. C., and A. L. Zydney, "Theoretical Analysis of the Effect of Membrane Morphology on Fouling during Microfiltration," *Sep. Sci. Technol.*, **34**, 2461 (1999).

Jakobs, E., and W. J. Koros, "Ceramic Membrane Characterization Via the Bubble Point Technique," *J. Membr. Sci.*, **124**, 149 (1997).

Kesting, R. E., "Characterization," *Synthetic Polymeric Membranes*, R. E. Kesting, ed., McGraw-Hill, New York (1971).

Kujawski, W., P. Adamczak, and A. Narebska, "A Fully Automated System for the Determination of Pore Size Distribution in Microfiltration and Ultrafiltration Membranes," *Sep. Sci. Technol.*, **24**, 495 (1989).

Mikulášek, P., and P. Dolecek, "Characterization of Ceramic Tubular Membranes by Active Pore-Size Distribution," *Sep. Sci. Technol.*, **29**, 1183 (1994).

Mulder, M., *Basic Principles of Membrane Technology*, Kluwer Academic, Dordrecht, The Netherlands (1991).

Munari, S., A. Bottino, G. Capannelli, and P. Moretti, "Membrane Morphology and Transport Properties," *Desalination*, **53**, 11 (1985).

Munari, S., A. Bottino, P. Moretti, G. Capannelli, and I. Becchi, "Permoporometric Study on Ultrafiltration Membranes," *J. Membr. Sci.*, **41**, 69 (1989).

Nakao, S. I., "Determination of Pore Size and Pore Size Distribution. 3. Filtration Membranes," *J. Membr. Sci.*, **96**, 131 (1994).

Piatkiewicz, W., S. Rosinski, D. Lewinska, J. Bukowski, and W. Judycki, "Determination of Pore Size Distribution in Hollow Fibre Membranes," *J. Membr. Sci.*, **153**, 91 (1999).

Vaidya, A. M., and N. J. Haselberger, "A Novel Technique for the Characterization of Asymmetric Membranes by Permoporometry," *Sep. Sci. Technol.*, **29**, 2523 (1994).

Wienk, I. M., B. Folkers, Th. van den Boomgaard, and C. A. Smolders, "Critical Factors in the Determination of the Pore Size Distribution of Ultrafiltration Membranes Using the Liquid Displacement Method," *Sep. Sci. Technol.*, **29**, 1433 (1994).

Manuscript received May 22, 2003, and revision received Sep. 5, 2003.